Talanta 81 (2010) 493–498

Contents lists available at ScienceDirect

Talanta

journal homepage: www.elsevier.com/locate/talanta

Enrichment and fluorescence enhancement of adenosine using aptamer–gold nanoparticles, PDGF aptamer, and Oligreen

Shih-Ju Chen[a], Chih-Ching Huang[b], Huan-Tsung Chang[a,*]

[a] Department of Chemistry, National Taiwan University, 1, Section 4, Roosevelt Road, Taipei 10617, Taiwan
[b] Institute of Bioscience and Biotechnology, National Taiwan Ocean University, 2, Pei-Ning Rd, Keelung 20224, Taiwan

ARTICLE INFO

Article history:
Received 13 November 2009
Received in revised form
17 December 2009
Accepted 17 December 2009
Available online 24 December 2009

Keywords:
Aptamer
Gold nanoparticles
Oligreen
PDGF aptamer

ABSTRACT

In this study, we have developed a simple, cost-effective, label-free fluorescence analytical assay – comprising an adenosine-binding aptamer (Apt_{Ado}), platelet-derived growth factor (PDGF)-binding aptamer (Apt_{PDGF}), gold nanoparticles (Au NPs), and the DNA-binding dye Oligreen (OG) – for the determination of adenosine. Apt_{Ado} and Apt_{PDGF} are for the recognition of adenosine and for the amplification of fluorescence signal, respectively. The presence of adenosine induces the conformational switch of the Apt_{Ado} from coiled to a G-quadruplex structure, leading to the less binding of Apt_{Ado} onto the surface of Au NPs. The more the adenosine is present, the less the amount of Apt_{Ado} is adsorbed, resulting in the fluorescence change of the aptamer–OG complexes. When using a mixture of Apt_{Ado} (15.0 nM), Au NPs (0.1 nM), and OG (0.05×) in 5.0 mM phosphate (pH 7.4), this sensor provides the limit of detection of 70.0 nM for adenosine at a signal-to-noise ratio of 3. The LOD for adenosine is down to 5.5 nM when using Apt_{Ado} modified Au NPs (Apt_{Ado}–Au NPs) and Apt_{PDGF} for the enrichment of adenosine and amplification of fluorescence signal of OG, respectively. The practicality of the present sensor has been validated by the determination of adenosine in diluted urine samples, showing its advantages of simplicity, selectivity, sensitivity, and minimal matrix interference.

1. Introduction

Aptamers are single-stranded DNA or RNA sequences selected in vitro through systematic evolution of ligands by exponential enrichment (SELEX) for the recognition of target analytes with high affinity and specificity [1,2]. Because aptamers often undergo conformational changes upon binding to their targets, several assays have been developed for biosensing of analytes of interest [3,4]. For example, assays based on fluorescence resonance energy transfer (FRET) using an aptamer labeled with an acceptor and a donor allow the sensing of small molecules, DNAs, proteins and metal ions under extracellular conditions [5–7].

Because adenosine is involved in the regulation of renal hemodynamics, tubular re-absorption, and the release of rennin, its determination is an important means of evaluating renal injury [8]. Radioimmunoassay, voltammetry, and high-performance liquid chromatography (HPLC) are most commonly applied to determine the concentrations of adenosine in real samples [9–11]. Although these methods are practical, they suffer from the need to pre-treat the sample, the need for large amounts of samples and reagents, low sensitivity, poor reproducibility, and/or safety risks. Recently, oligonucleotides containing guanine-rich sequences, which fold into G-quadruplexes in the presence of their target analytes, have been employed to recognize adenosine and its phosphorylated derivatives (e.g., ATP) based on colorimetric, fluorescence, and electrochemical detection [12–19]. Although sensing systems usually suffer from more serious matrix interference effects than separation approaches, they do not use large amounts of solvents and reagents. Fluorescence-signaling aptamers have been used as sensing probes, with advantages of rapidity, sensitivity, and versatility [15,16,20–23]. An aptamer beacon derivatized with fluorescein and 4-(4-dimethylaminophenylazo)benzoic acid has been employed for the detection of ATP based on structural switching from a DNA–DNA duplex to a DNA–target complex, leading to fluorescence dequenching [20]. One drawback is that labeling is always required to transduce the aptamer recognition events to detectable fluorescent signals, which complicates the process, as well as increases the assay's cost and the probability of interference from undesired side products.

Labeled or modified aptamers are reported to show weaker binding to the target as compared to that for unmodified aptamers [20]. To minimize this disadvantage, simple label-free probes using DNA intercalating dyes or photoactive polymers have been designed to report the recognition and binding between an aptamer and target molecule [24–28]. For example, an aptamer sensor – which is not modified with an extrinsic fluorophore – has been

* Corresponding author. Tel.: +886 2 33661171; fax: +886 2 33661171.
E-mail address: changht@ntu.edu.tw (H.-T. Chang).

0039-9140/$ – see front matter © 2009 Elsevier B.V. All rights reserved.
doi:10.1016/j.talanta.2009.12.030

prepared for the detection of ATP by its target-induced conformational change leading to a significant luminescence change of $[Ru(phen)2(dppz)]^{2+}$ [24]. A similar strategy has been developed for ATP detection using ethidium bromide and light harvesting cationic tetrahedralfluorene that is used to further enhance the dye emission through energy transfer [26]. Nevertheless, these methods suffer from several limitations, such as high background and lower sensitivity.

Since the analyte level in real samples can be very low, aptamer-based biosensors are desirable with high sensitivity and selectivity. For example, gold nanoparticles (Au NPs) conjugated with aptamers have been used for improving the sensitivity of electrochemical or optical sensors for the determination of adenosine [15,19,29–31]. In this study, we demonstrated a simple, label-free fluorescence sensor using adenosine-binding aptamer (Apt_{Ado}), Au NPs, and Oligreen (OG) for adenosine detection. Upon adenosine binding, the conformational changes in the Apt_{Ado} resulted in the less binding of aptamer–OG complexes on each Au NP, leading to a significant adenosine-dependent fluorescence change. We evaluated the effect of the size of Au NPs, and the surface density of Apt_{Ado} on the determination of adenosine. To further improve the sensitivity, we used the Apt_{Ado} modified Au NPs (Apt_{Ado}–Au NPs) and platelet-derived growth factor (PDGF)-binding aptamer (Apt_{PDGF}) to enrich adenosine, leading to improve its sensitivity. To demonstrate the practicality, the present approach was applied to the determination of adenosine in human urine sample. Based on the fact that different aptamers can undergo conformational change toward various analytes, this fundamental concept opens a new avenue for designing sensors for other important analytes.

2. Experimental

2.1. Chemicals

Sodium tetrachloroaurate(III) dehydrate, adenosine, uridine, guanosine, and cytidine were obtained from Sigma (St. Louis, MO). OliGreen (OG) was obtained from Molecular Probes (Portland, OR). Because the manufacturer did not provide the concentration of OG, the concentration of OG is herein defined as 100×. The OG was diluted 100-fold with 5 mM phosphate (pH 7.4) solution prior to use. The 5′-thiol-modified adenosine-binding aptamer (5′ HS-TTT TTT ACC TGG GGG AGT ATT GCG GAG GAA GGT-3′) [32,33], 5′-thiol-modified PDGF-binding aptamer (5′ HS-CAG GCT ACG GCA CGT AGA GCA TCA CCA TGA TCC TG-3′) [34], and 24-nt poly(T) were purchased from Integrated DNA Technologies, Inc. (Coralville, IA). All of the other reagents used in this study were purchased from Aldrich (Milwaukee, WI).

2.2. Synthesis of 13-, 32-, and 56-nm Au NPs

Au NPs were prepared by the reduction of sodium tetrachloroaurate with trisodium citrate that also acted as a capping agent to stabilize the as-prepared Au NPs. By carefully controlling the amount of citrate in the synthesis process, different sizes of Au NPs were synthesized [35]. Trisodium citrate solutions [1% (w/v); 0.8, 0.5, and 0.3 mL] were added separately and rapidly to three respective aliquots of 0.01% $NaAuCl_4$ solutions that were heated under reflux. The mixtures (final volumes: 50 mL each) were heated under reflux for an additional 8 min, during which time the color changed to deep red, wine red, and pale red, respectively. The sizes of the nanoparticles were verified by transmission electron microscopy (TEM) (H7100, Hitachi High-Technologies Corp., Tokyo, Japan); they appeared to be nearly monodispersed, with an average size of 13.3 (±1.2), 32.2 (±2.9), and 56.2 (±5.1) nm, respectively (Fig. S1). A double beam UV–vis spectrophotometer (Cintra 10e) from GBC (Victoria, Australia) was used to measure the absorption of the Au NPs solutions. The UV–Vis absorption spectra (data not shown) display maximum wavelengths of the surface plasmon resonance (SPR) bands of the 13-, 32-, 56-nm Au NPs at 518, 526, and 535 nm, respectively. Based on the absorbance values, we estimated that the concentrations of the 13-, 32-, and 56-nm Au NPs to be about 2.4×10^{12}, 1.6×10^{11}, and 3.0×10^{10} particles/mL, respectively [35].

2.3. Fluorescence detection of adenosine

Aliquots (20.0 μL) of 5.0 mM sodium phosphate (pH 7.4) solutions containing 15.0 nM Apt_{Ado} in the presence of adenosine (0–1.0 μM) were equilibrated at room temperature for 30 min. The 32-nm Au NPs were then added to the solutions to obtain a final concentration of 0.1 nM Au NPs and the mixtures (190.0 μL) were equilibrated again for 30 min. Prior to measuring the fluorescence, aliquots (10.0 μL) of an OG solution (0.05×) were added to the solutions and the mixtures were then equilibrated for 10 min. The mixtures were then transferred into 0.4-mL quartz cuvettes. The fluorescence spectra were recorded using a Cary Eclipse fluorescence spectrophotometer from Varian (CA, USA) operated at an excitation wavelength of 480 nm.

2.4. Preparation of aptamer-bound 32-nm Au NPs

Aliquots of the as-prepared 32-nm Au NP solutions (990.0 μL) in 1.5 mL tubes were mixed separately with the Apt_{Ado} (150.0–300.0 nM, 10.0 μL) to obtain a final concentration of 0.25 nM Au NPs and final concentrations of 15.0, 22.5 and 30.0 nM Apt_{Ado}. After incubation for 24 h at room temperature, the mixtures were centrifuged for 15 min at 12,000 rpm to remove the excess thiol-DNA. Following removal of the supernatants, the oily precipitates were washed with 4.0 mM trisodium citrate. After two wash/centrifuge cycles, the Apt_{Ado}–Au NPs was resuspended separately in 4.0 mM trisodium citrate and stored in a refrigerator (4 °C). To determine the number of Apt_{Ado} molecules on each Au NP, the amount of Apt_{Ado} in the supernatant after centrifugation was measured using OG.

2.5. Apt_{PDGF}/Apt_{Ado}–Au NPs sensor for adenosion determination

Aliquots (184.0 μL) of 5.0 mM sodium phosphate (pH 7.4) solutions containing the 0.1 nM Apt_{Ado}–Au NPs (32 nm) in the presence of adenosine (0–300.0 nM) were equilibrated at room temperature for 30 min. The 6.0 μL Apt_{PDGF} (100.0 nM) prepared in 1.0 M NaCl were then added to the solutions and the mixtures were equilibrated again for 30 min. Prior to measuring the fluorescence, aliquots (10.0 μL) of an OG solution (0.05×) were added to the solutions and the mixtures were then equilibrated for 10 min. The mixtures were then transferred into 0.4-mL quartz cuvettes. The fluorescence spectra were recorded using fluorescence spectrophotometer operated at an excitation wavelength of 480 nm.

2.6. Preparation and analysis of urine samples

Freshly voided urine samples were obtained from a healthy female volunteer. Each sample was filtered through a 0.2-mm membrane to remove particulate matter. Aliquots of human urine samples (2.0 μL) were spiked with standard solutions of adenosine (2.0 μL) and were then diluted to 184.0 μL using 5.0 mM phosphate buffer (pH 7.4) containing, 0.1 nM Apt_{Ado}–Au NPs. The 6.0 μL Apt_{PDGF} (100.0 nM) prepared in 1.0 M NaCl was added to the mixtures after the incubation at 25 °C for 30 min. After being subjected to further equilibration for 30 min, 0.05× OG was then added to each solution. The final concentrations of the spiked adenosine

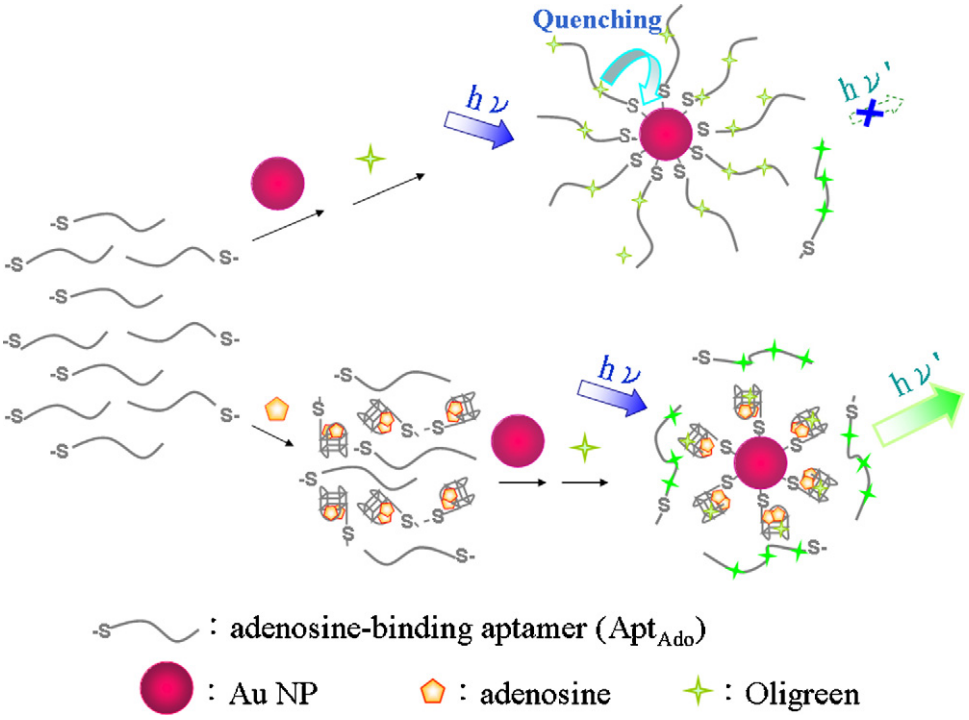

Scheme 1. Schematic representation of the label-free adenosine sensor based on the target-induced conformational change of aptamer. The sensor solution contains Apt_{Ado}, OG, and Au NPs.

were over the range 10.0–40.0 nM. The fluorescence of each of the solutions was recorded after equilibration for 10 min.

3. Results and discussion

3.1. Sensing strategy of OG-Apt_{Ado}/Au NP

We developed a simple, cost-effective, label-free fluorescence assay – comprising Apt_{Ado}, Au NPs, and the DNA-binding dye OG – for the determination of adenosine (Scheme 1) through fluorescence quenching mediated by Au NPs via FRET, electron transfer, and/or collision processes [36–38]. In the absence of adenosine, the aptamer molecules possess a random-coiled single-stranded DNA (ssDNA) structure and bind to Au NPs through strong Au–S interactions. As a result, only a few aptamer molecules exist in the bulk solution and, therefore, most of the OG molecules bind with the aptamers bound to the Au NP surfaces. The fluorescence is weak because the Au NPs cause fluorescence quenching of OG–aptamer complexes on their surface. Since the aptamer we used binds two adenosine molecules in a non-canonical, but stable, helix comprised of G:G and G:A base pairs flanked by short canonical helices [33]. Upon binding to adenosine, the aptamer changes its conformation from a loose random-coil ssDNA to a rigid tertiary structure. Because steric effects occur on the Au NP surfaces, the number of adenosine–aptamer complexes is fewer than that of the random-coil aptamers. In other words, there are more aptamer molecules available to interact with OG in the bulk solution, leading to greater fluorescence in the presence of adenosine.

3.2. OG-Apt_{Ado}/Au NP-based sensor for adenosine

We performed proof-of-concept experiments by adding the aptamer (0.3 μM, 10.0 μL) into 32-nm Au NP solutions (0.25 nM, 80.0 μL) in the presence and absence of adenosine (1.0 μM) to obtain a final volume of 200.0 μL. Fig. 1 displays the fluorescence spectra of the mixtures and a control solution, namely OG (0.05×) in 5.0 mM sodium phosphate buffer (pH 7.4). Since OG is weakly fluorescent, but exhibits a great enhancement in its fluorescence upon binding to ssDNA. It is a sensitive fluorescent nucleic acid stain for quantitating ssDNA in solution. OG is ca. 500-fold more sensitive than ethidium bromide (EtBr) for the detection of DNA [39]. Curve a reveals the negligible fluorescence of the OG (0.05×) solution. Curve b indicates that the fluorescence intensity at 524 nm of the OG solution (0.05×), when excited at 480 nm, increased by a factor of greater than 200-fold after the addition of 15.0 nM random-coil Apt_{Ado}. The fluorescence intensity of the aptamer–OG complex increased linearly ($R^2 > 0.99$) upon increasing the concen-

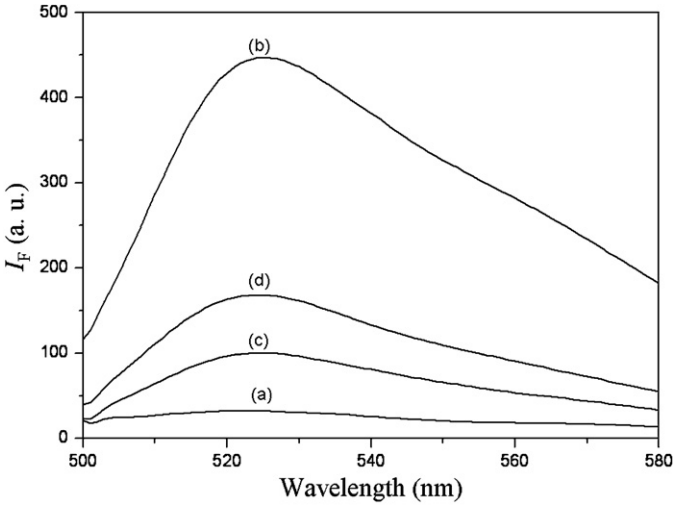

Fig. 1. Fluorescence spectra (λ_{ex} 480 nm) of (a) OG solution; (b) mixtures of OG and aptamer; (c) and (d) supernatants of mixtures of 32-nm Au NPs, aptamer, and OG in the (c) absence and (d) presence of adenosine (1 μM). The concentrations of aptamer, 32-nm Au NPs and OG were 15.0 nM, 0.1 nM and 0.05×, respectively. Solutions were prepared in 5.0 mM phosphate (pH 7.4). The fluorescence intensities (I_F) are plotted in arbitrary units (a.u.).

Table 1
Comparison of different sizes of Au NPs for the analysis of adenosine.

	Au NPs (nm)		
	13	32	56
Number of Au NPs ($\times 10^{10}$ particles/mL)	36	6	2
Surface area (nm^2/particle)	531	3217	9852
Total surface area ($\times 10^{14}$ nm^2/mL)	2	2	2
Aptamer molecules per Au NP particle	25	120	330
	Determination of adenosine		
Dynamic range (μM)	0–1.0	0–1.0	0–0.8
Regression coefficient (R^2)	0.99	0.99	0.98
LOD (nM)	110.0	70.0	170.0

tration of the aptamer from 0.5 to 15.0 nM (data not shown). Our results suggest that the use of OG to label the oligonucleotides not only produces a large increase in the fluorescent intensity but also minimizes the degree of background interference. In addition, we investigated the effect of adenosine concentration on the fluorescence intensity of aptamer-OG mixtures (Fig. S2). The fluorescence intensity slightly decreased in the presence of adenosine; about an 8% decrease in the presence of 1.0 μM adenosine. Since OG binds to single- and double-stranded DNA, the changes in the fluorescence of the aptamer-OG mixtures induced by adenosine were not significant because of a high background signal. To minimize background signals, Au NPs were used in this study. In the presence of the Au NPs, a significant decrease in the fluorescence intensity occurred (curve c), supporting our notion that the aptamer molecules bind to the Au NP surfaces and that the Au NPs exhibit a high fluorescence quenching efficiency [34]. We also performed the following experiment to confirm the effective binding of the aptamer to the Au NPs. A mixture of the Au NPs, aptamer, and OG was subjected to centrifugation at 12,000 rpm for 10 min. From the fluorescence intensity of supernatant, we estimated ~84% of the aptamer molecules were bound to Au NPs. In the presence of adenosine, the mixture of the aptamer, Au NPs, and OG fluoresced strongly (curve d). The fluorescence intensity was ca. 32% that of curve b, revealing that there were more aptamer molecules (ca. 16%) existed in the bulk solution. Since the binding of the dye OG to ssDNA is non-specific, an additional control experiment was performed by adding the 24-nt, random-sequenced ssDNA to the mixture of OG, and adenosine. In the control experiments, there was no obvious difference of fluorescence intensity of probe solutions in the absence and presence of adenosine (1.0 μM).

3.3. Effect of particle sizes

We investigated the effect of the size of the Au NPs on the determination of adenosine. We varied the sizes and concentrations of three different Au NP solutions – 13-nm (0.6 nM), 32-nm (0.1 nM), and 56-nm (0.04 nM) Au NPs – to maintain the total surface area of Au NPs in each solution at a constant value. Because the fluorescence intensities of the three mixtures in the absence of adenosine were different, we plotted $(I_F - I_{F0})/I_{F0}$ ratios to compare the impact of Au NP size on the sensitivity of the sensor toward adenosine, where I_{F0} and I_F represent the fluorescence intensities of the mixtures in the absence and presence of the adenosine, respectively. Fig. 2 reveals that, from a plot of the $(I_F - I_{F0})/I_{F0}$ ratios of the three mixtures against the adenosine concentration, the greatest sensitivity occurred when using the 32-nm Au NP solution. Table 1 summarizes the results. The LODs for adenosine when using the 13-, 32-, and 56-nm Au NP solutions were 110.0, 70.0, and 170.0 nM, respectively. The sensitivity is comparable or better than those obtained by the most reported fluorescence assays [20,24,26]. We estimated the average number of aptamer molecules on each of these three types of Au NPs to be 25, 120, and 330, respectively.

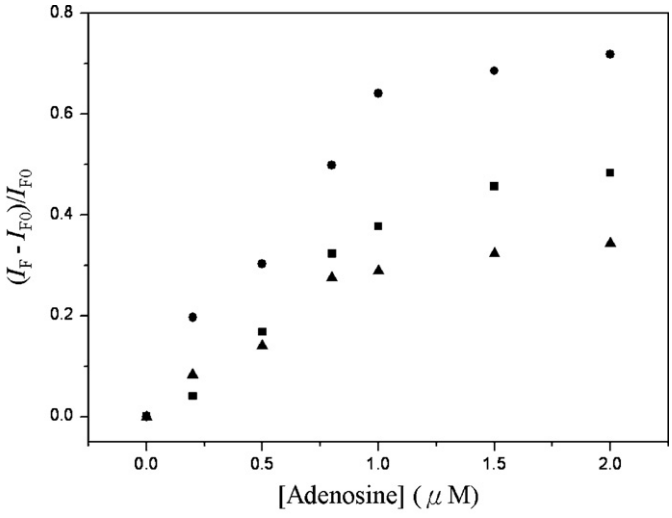

Fig. 2. The fluorescence signal increase ratio $(I_F - I_{F0})/I_{F0}$ of the aptamer–OG complex upon increasing the concentration of adenosine in 13-nm (square), 32-nm (circle), and 56-nm (triangle) Au NPs solutions, respectively. I_{F0} and I_F are the fluorescence intensities of the aptamer–OG complex in the absence and presence of adenosine, respectively. Other conditions were the same as those described in Fig. 1.

When using small Au NPs, the greater number and faster collisions (higher concentrations and diffusion coefficients) of the Au NPs caused a greater degree of fluorescence quenching, leading to poorer sensitivity. On the other hand, the less sensitivity obtained by using the 56-nm Au NPs was mainly due to the greater degree of quenching arising from the formation of large aggregates. The 56-nm Au NPs were not as stable as the two smaller congeners, and thus, the probe provided relatively poor reproducibility. In addition, the less surface curvature of larger size Au NPs retards the access of the aptamer onto their surfaces [40–42]. Based on all the values listed in Table 1, we conclude that the 32-nm Au NP solution provided superior analytical performance relative to the other two solutions.

3.4. Sensitivity improvement of aptamer-based nanosensor

To further improve the sensitivity of our aptamer-based sensor, we used NPs to assist the binding efficiency between Apt_{Ado} and adenosine (Scheme 2). It was known that when aptamers immobilized on the surface of Au NPs, the binding constant provided large than one order of magnitude higher than which in the free solution, that is likely due to the multivalent binding effect (ultra-high densities of Apt on the local surface of Au NPs) [34]. We used Apt_{Ado}–Au NPs to selectively concentrate adenosine from the solution and used Apt_{PDGF} to obtain greater fluorescence signals. We note that Apt_{PDGF} could not easily replace the Apt_{Ado} molecules on the Au NP surfaces within 1 h; it took about 18 h for the exchange reaction to occur. We pointed out that the Apt_{PDGF} molecules interacted more strongly than the Apt_{Ado} with OG; the fluorescence ratio of the complexes of OG (0.05×) with Apt_{PDGF} and with Apt_{Ado} (both 10.0 nM) was about 2.1 (data not shown) Unlike the Apt_{Ado} formed a random-coil structure, the Apt_{PDGF} formed a three-way helix junction with a conserved single-stranded loop at the branch point and thus they were more difficult to access to the surfaces of Apt_{Ado}–Au NPs [43]. To stabilize the three-way helix structure of Apt_{PDGF} while minimizing salt induce fluorescence quenching and instability of Au NPs, 30.0 mM NaCl was essential in the mixture [43,44]. Once aptamer molecules on the Au NP surfaces interacted with adenosine, they changed from randomly coiled structure to G-quadruplexes. Because of steric effects due to the formation of G-quadruplexes, it is even more difficult for the Apt_{PDGF} to access

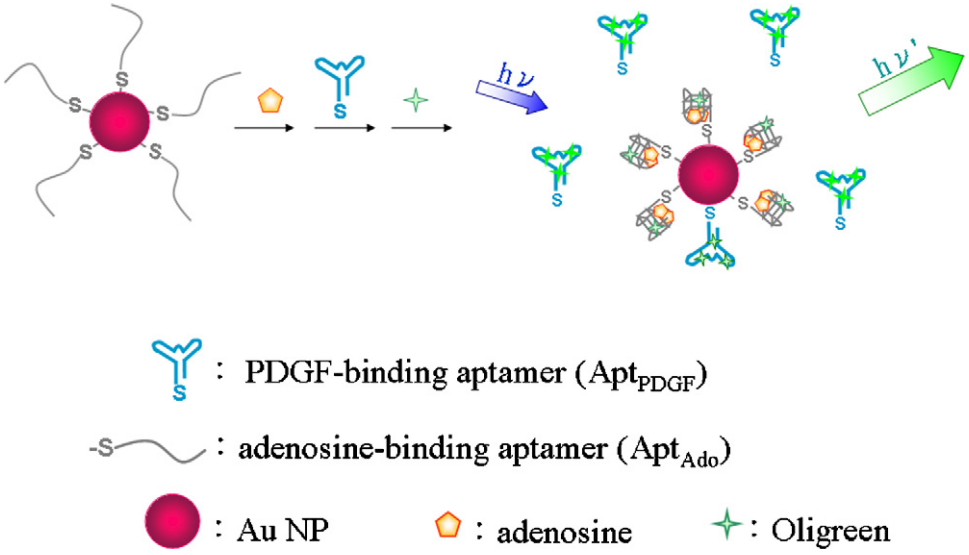

Scheme 2. Schematic representation of the sensing assay using Apt$_{Ado}$–Au NPs and Apt$_{PDGF}$ to improve the sensitivity. The sensor solution contains Apt$_{Ado}$–Au NPs, Apt$_{PDGF}$, and OG.

to the surface of the Apt$_{Ado}$–Au NPs. As a result, upon increasing the concentration of adenosine there were more Apt$_{PDGF}$ molecules in the bulk solution, leading to stronger fluorescence. We note that these unbound Apt$_{PDGF}$ molecules in the solution relative to those on the Au NP surfaces have stronger fluorescence. To find the optimum condition of the Apt$_{Ado}$–Au NPs probe for adenosine binding, we tested Au NPs having different Apt$_{Ado}$ densities on the surface in the presence of Apt$_{PDGF}$ (1–10.0 nM) (Fig. S3). For simplicity, we denote the three Apt$_{Ado}$–Au NPs having 60-, 90-, and 120-Apt$_{Ado}$ molecules per Au NP as 60-, 90-, and 120-Apt$_{Ado}$–Au NPs, respectively. In general, low-density aptamer molecules on the surface were more likely to exist in flattened structures as a result of strong interactions with the Au surfaces [45]. Thus, the efficiency of capturing the adenosine from bulk solution was relatively low. On the other hand, high-density aptamer molecules on the Au NPs surface would be too crowded to be folded to form well characterized G-quadruplex structures. In addition, it is more difficult for the Apt$_{PDFG}$ to access to the Au NP surfaces, and therefore impairing the fluorescence enhancement. On the basis of our results, the 90-Apt$_{Ado}$–Au NPs in the presence of 3.0 nM Apt$_{PDGF}$ provided the best sensitivity, mainly because of low fluorescence background signal and greater fluorescence signals.

Next, we used the 90-Apt$_{Ado}$–Au NPs to determine adenosine in solutions consisting of 3.0 nM Apt$_{PDGF}$, 30.0 mM NaCl and 5 mM phosphate (pH 7.4). The fluorescence ratio of various adenosine solutions were depicted as shown in Fig. 3. These show that the fluorescence responses increased upon increasing adenosine concentration. The linear relationship of the signal enhancement ratios $(I_F - I_{F0})/I_{F0}$ against adenosine concentration as shown in Fig. 3 was from 10.0 to 200.0 nM, with the correlation coefficient of 0.97 and the LOD at S/N 3 of adenosine experimentally determined to be 5.5 nM. This Apt$_{Ado}$–Au NP-assisted adenosine enrichment and Apt$_{PDGF}$-aided fluorescence enhancement provided at least 12-fold sensitivity enhancement (5.5 nM vs. 70 nM) relative to that without conducting enrichment and signal amplification (Section 3.3).

3.5. Selectivity of OG-Apt$_{Ado}$/Au NP sensor for adenosine

Under the optimum conditions (0.1 nM 90-Apt$_{Ado}$–Au NPs, 3.0 nM Apt$_{PDGF}$, and 0.05× OG in 5.0 mM phosphate containing 30.0 mM NaCl), the selectivity toward adenosine against to other nucleotide bases (uridine, guanosine, and cytidine; each 1.0 μM) are exhibited in Fig. S4. As expected, uridine, guanosine, and cytidine did not cause significant increases in fluorescence because they do not induce the required structural switching of the aptamer. The selectivity values of this probe for adenosine over uridine, guanosine, and cytidine were 118.9, 60.2, and 55.6, respectively.

3.6. Urine analysis

To determine the practical potential of our sensor system for the analysis of adenosine in real biological samples, we determined the adenosine concentrations in urine samples because urinary adenosine is a sensitive marker of renal functional impairment [46]. Five aliquots of the purified sample solution (ca. 2.0 μL) were separately added to the sensing mixtures (5.0 mM phos-

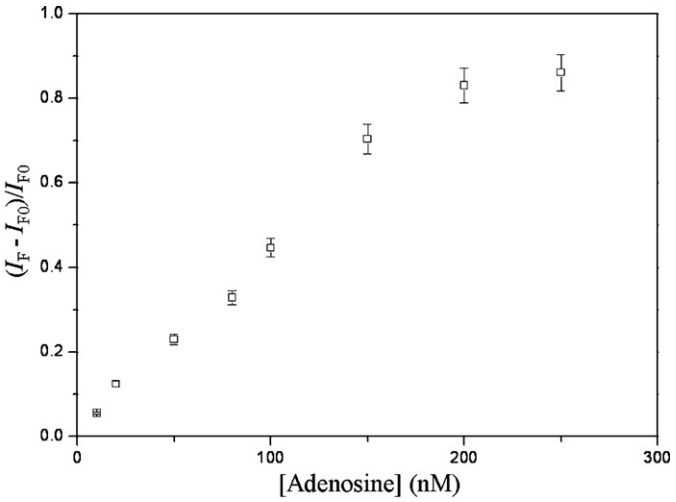

Fig. 3. Responses in the ratio $(I_F - I_{F0})/I_{F0}$ of 90-Apt$_{ado}$–Au NP solutions after the addition of adenosine at concentrations of 0, 10.0, 20.0, 50.0, 80.0, 100.0, 150.0, 200.0 and 300.0 nM. The concentrations of 90-Apt$_{Ado}$–Au NPs, Apt$_{PDGF}$ and OG were 0.1 nM, 3.0 nM and 0.05×, respectively. Solutions were prepared in 5.0 mM phosphate (pH 7.4) containing 30.0 mM NaCl. Error bars are standard deviations based on three independent measurements.

phate buffer containing 30.0 mM NaCl, 0.1 nM 90-Apt_{Ado}–Au NPs, 3.0 nM Apt_{PDGF}, and 0.05× OG), each with 100-fold dilution. Dilution is quite important to minimize the matrix interference and to reduce salt induced aggregation of the 90-Apt_{Ado}–Au NPs. From the addition of adenosine standards, we determined the adenosine concentration based on the linear plot of $(I_F - I_{F0})/I_{F0}$ against the spiked adenosine concentration over the range 0–40.0 nM ($y = 0.225 + 0.007x$, $R^2 = 0.98$, in which x and y are the concentration (nM) of spiked adenosine and fluorescence ratio, respectively) (Fig. S5). Our sensor system provided good recovery (95.6–97.3%) of the diluted samples spiked with adenosine. The concentration of adenosine in one representative urine sample was 3.2 ± 0.2 μM ($n = 3$), which agrees well with the levels normally found in human urine (2.0–7.0 μM) [47,48]. We point out that the probe without containing 3.0 nM Apt_{PDGF} could not be used for the determination of adenosine, mainly because of its poor sensitivity. Although concentration of the analyte through solid phase extraction prior to analysis using the probe without containing 3.0 nM Apt_{PDGF} is practical, it is not as simple as the present approach.

4. Conclusions

In conclusion, we have developed a simple, homogeneous, cost-effective, sensitive, and selective fluorescence sensor for the determination of adenosine in urine. We used two different aptamers—Apt_{ado} for the recognition of adenosine and Apt_{PDGF} for signal amplification. The sensitivity was highly dependent on the fluorescence of the aptamer–OG complexes, the quenching efficiency of the Au NPs, and the density of the aptamer–OG complexes on each Au NP, which is strongly related to the concentration of adenosine required to induce the conformational change of the aptamer from coiled to a tertiary structure. Using the Apt_{ado}–Au NPs nanosensor, we determined the levels of adenosine in urine samples without the need for pre-treatment. This fundamental concept opens a new avenue for designing sensors for other important analytes, such as Hg^{2+}, thrombin, and S-adenosylmethionine.

Acknowledgements

We are grateful to the National Science Council of Taiwan for providing financial support to this study under contracts NSC 98-2627-M-002-013, NSC 98-2627-M-002-014, and NSC 98-2113-M-002-011-MY3.

Appendix A. Supplementary data

Supplementary data associated with this article can be found, in the online version, at doi:10.1016/j.talanta.2009.12.030.

References

[1] C. Tuerk, L. Gold, Science 249 (1990) 505.
[2] A.D. Ellington, J.W. Szostak, Nature 346 (1990) 818.
[3] N.K. Navani, Y. Li, Curr. Opin. Chem. Biol. 10 (2006) 272.
[4] C.C. Huang, H.T. Chang, Chem. Commun. 2008 (2008) 1461.
[5] S. Nagatoishi, T. Nojima, E. Galezowska, A. Gluszynska, B. Juskowiak, S. Takenaka, Anal. Chim. Acta 581 (2007) 125.
[6] P.C. Ray, G.K. Darbha, A. Ray, J. Walker, W. Hardy, Plasmonics 2 (2007) 173.
[7] Y.C. Huang, B. Ge, D. Sen, H.Z. Yu, J. Am. Chem. Soc. 130 (2008) 8023.
[8] V. Vallon, B. Muhlbauer, H. Osswald, Physiol. Rev. 86 (2006) 901.
[9] H.M. Siragy, J. Linden, Hypertension 27 (1996) 404.
[10] R.N. Goyal, V.K. Gupta, S. Chatterjee, Talanta 76 (2008) 662.
[11] G. Luippold, U. Delabar, D. Kloor, B. Muhlbauer, J. Chromatogr. B 724 (1999) 231.
[12] J. Liu, Y. Lu, Adv. Mater. 18 (2006) 1667.
[13] W. Zhao, W. Chiuman, M.A. Brook, Y. Li, ChemBioChem 8 (2007) 727.
[14] S.J. Chen, Y.F. Huang, C.C. Huang, K.H. Lee, Z.H. Lin, H.T. Chang, Biosens. Bioelectron. 23 (2008) 1749.
[15] B. Juskowiak, Anal. Chim. Acta 568 (2006) 171.
[16] Z. Tang, P. Mallikaratchy, R. Yang, Y. Kim, Z. Zhu, H. Wang, W. Tan, J. Am. Chem. Soc. 130 (2008) 11268.
[17] S. Zhang, J. Xia, X. Li, Anal. Chem. 80 (2008) 8382.
[18] Z.S. Wu, M.M. Guo, S.B. Zhang, C.R. Chen, J.H. Jiang, G.L. Shen, R.Q. Yu, Anal. Chem. 79 (2007) 2933.
[19] M. Zayats, Y. Huang, R. Gill, C.A. Ma, I. Willner, J. Am. Chem. Soc. 128 (2006) 13666.
[20] R. Nutiu, Y. Li, J. Am. Chem. Soc. 125 (2003) 4771.
[21] N. Rupcich, R. Nutiu, Y. Li, J.D. Brennan, Anal. Chem. 77 (2005) 4300.
[22] R. Nutiu, Y. Li, Methods 37 (2005) 16.
[23] M. Levy, S.F. Cater, A.D. Ellington, ChemBioChem 6 (2005) 2163.
[24] J. Wang, Y. Jiang, C. Zhou, X. Fang, Anal. Chem. 77 (2005) 3542.
[25] F. He, Y. Tang, S. Wang, Y. Li, D. Zhu, J. Am. Chem. Soc. 127 (2005) 12343.
[26] Y. Wang, B. Liu, Analyst 133 (2008) 1593.
[27] H. Wei, B. Li, J. Li, E. Wang, S. Dong, Chem. Commun. 2007 (2007) 3735.
[28] H.A. Ho, M. Leclerc, J. Am. Chem. Soc. 126 (2004) 1384.
[29] Y. Du, B. Li, H. Wei, Y. Wang, E. Wang, Anal. Chem. 80 (2008) 5110.
[30] J. Wang, H.S. Zhou, Anal. Chem. 80 (2008) 7174.
[31] J. Wang, A. Munir, H.S. Zhou, Talanta 79 (2009) 72.
[32] D.E. Huizenga, J.W. Szostak, Biochemistry 34 (1995) 656.
[33] C.H. Lin, D.J. Patei, J. Chem. Biol. 4 (1997) 817.
[34] C.C. Huang, S.H. Chiu, Y.F. Huang, H.T. Chang, Anal. Chem. 79 (2007) 4798.
[35] Y.F. Huang, H.T. Chang, Anal. Chem. 78 (2006) 1485.
[36] P.V. Kamat, S. Barazzouk, S. Hotchandani, Angew. Chem., Int. Ed. 41 (2002) 2764.
[37] E. Dulkeith, A.C. Morteani, T. Niedereichholz, T.A. Klar, J. Feldmann, S.A. Levi, F. Van Veggel, D.N. Reinhoudt, M. Moller, D.I. Gittins, Phys. Rev. Lett. 89 (2002) 203002.
[38] T. Huang, R.W. Murray, Langmuir 18 (2002) 7077.
[39] R.P. Haugland, M.T.Z. Spence, I.D. Johnson, in: B.M.T.Z. Spence (Ed.), The Handbook: A Guide to Fluorescent Probes and Labeling Technologies, Invitrogen Corp., Molecular Probes, Carlsbad CA, 2005, p. 357.
[40] E. Roduner, Chem. Soc. Rev. 35 (2006) 583.
[41] A.C. Templeton, W.P. Wuelfing, R.W. Murray, Acc. Chem. Res. 33 (2000) 27.
[42] K.H. Lee, S.J. Chen, J.Y. Jeng, Y.C. Cheng, J.T. Shiea, H.T. Chang, J. Colloid Interface Sci. 307 (2007) 340.
[43] L.S. Green, D. Jellinek, R. Jenison, A. Ostman, C.H. Heldin, N. Janjic, Biochemistry 35 (1996) 14413.
[44] J. Floege, T. Ostendorf, U. Janssen, M. Burg, H.H. Radeke, C. Vargeese, S.C. Gill, L.S. Green, N. Janjic, Am. J. Pathol. 154 (1999) 169.
[45] C.W. Liu, C.C. Huang, H.T. Chang, Langmuir 24 (2008) 8346.
[46] N. Heyne, P. Benohr, B. Muhlbauer, U. Delabar, T. Risler, H. Osswald, Nephrol. Dial. Transplant. 19 (2004) 2737.
[47] D. Kloor, K. Yao, U. Delabar, H. Osswald, Clin. Chem. 46 (2000) 537.
[48] H. Taniai, S. Sumi, T. Ito, A. Ueta, Y. Ohkubo, H. Togari, Tohoku J. Exp. Med. 208 (2006) 57.